Fusion Engineering and Design 190 (2023) 113530

Contents lists available at ScienceDirect

Fusion Engineering and Design

journal homepage: www.elsevier.com/locate/fusengdes

Thermomechanical analysis of a multi-reflectometer system for DEMO

Y. Nietiadi [a,*], R. Luís [a], A. Silva [a], J.H. Belo [a], A. Vale [a], A. Malaquias [a], B. Gonçalves [a], F. da Silva [a], J. Santos [a], E. Ricardo [a], W. Biel [b,c]

[a] Instituto de Plasmas e Fusão Nuclear, Instituto Superior Técnico, Universidade de Lisboa, Av. Rovisco Pais 1, 1049-001 Lisboa, Portugal
[b] Forschungszentrum Jülich GmbH, Institute of Energy and Climate Research, 52428 Jülich, Germany
[c] Department of Applied Physics, Ghent University, Belgium

ARTICLE INFO

Keywords:
DEMO
Diagnostics
Reflectometry
Thermomechanical
ANSYS

Microwave reflectometry systems are currently considered as a possible solution for plasma position and control, in DEMO. The primary integration approach for this diagnostic involves the incorporation of several groups of antennas and waveguides into a diagnostics slim cassette (DSC), a full 20–25 cm thick poloidal sector dedicated to diagnostics. Since the passive front-end components of the reflectometry system (antennas and WGs) will be directly exposed to the plasma, an effective cooling system is required to keep the operating temperatures below the limits established for the DSC materials under neutron irradiation. Furthermore, the mechanical stresses experienced by the DSC should not jeopardize its structural integrity. In this work, the temperature distributions of a DSC segment with an updated cooling system design were estimated with a coupled steady-state thermal analysis performed with ANSYS Mechanical and ANSYS CFX, using the system-coupling module of ANSYS Workbench. It was found that the maximum temperature obtained in the DSC could be below the limits if the antennas are made of tungsten. These results were used as input in structural analysis, which has shown that the structure of the designed DSC fulfils the level-A requirements of RCC-MR for Immediate Plastic Collapse (IPC), Immediate Plastic Instability (IPI), and Immediate Plastic Flow Localization (IPFL).

1. Introduction

Microwave (MW) reflectometry has been recently proposed as a suitable backup for magnetics diagnostics, the main tool for plasma equilibria real-time monitoring in DEMO [1]. In DEMO, reflectometry is expected to perform plasma density measurements in the gradient region, to determine the shape and the position of the plasma [2]. The implementation of the reflectometry system requires the front-end antennas to be exposed to the plasma. Therefore, they are foreseen to be made of EUROFER, with the possible addition of tungsten coating [3]. However, it was found in recent studies that in order to keep the erosion below 10 μm/year the antenna should be retracted 100 mm from the breeding blanket (BB) first wall (FW) [4].

The primary integration approach for the reflectometry system in DEMO is based on the Diagnostics Slim Cassette (DSC) concept, a full 20–25 cm thick poloidal sector dedicated to diagnostics to be integrated with the Water-Cooled Lithium Lead (WCLL) Breeding Blankets [5]. As EUROFER is the main material foreseen for the DSC housing several waveguides (WGs), a simple but effective cooling system is mandatory to keep the operating temperatures below the maximum allowable temperature for EUROFER under plasma operation (550 °C) [6].

This paper presents the results of thermomechanical analysis of a segment of the DSC inboard (IB) at the equatorial level, presented in Fig. 1, performed for a new design of the DSC, using ANSYS Workbench v19.1 [7]. Previous analyses [8,9] had shown that the DSC cooling system design had not successfully kept the DSC operating temperature under 550 °C in some particular regions (see Fig. 2); as such, the cooling system studied in the present work was designed to improve its performance, focusing on the removal of hotspots around the antenna cavities.

2. Workflow and simulation tools

Fig. 3 illustrates the steps followed to perform the simulations. The baseline design of the DSC created in a previous work [8] was imported to ANSYS SpaceClaim [7] and used to optimize the cooling channel design performance. As several important features of the case are kept the same, such as the plasma shape, DSC outer surfaces, and plasma power density, their calculation results (plasma thermal radiation and nuclear heat loads, obtained with MCNP [10]) are still relevant and

* Corresponding author.
E-mail address: ynietiadi@ipfn.tecnico.ulisboa.pt (Y. Nietiadi).

https://doi.org/10.1016/j.fusengdes.2023.113530
Received 10 October 2022; Received in revised form 6 January 2023; Accepted 31 January 2023
Available online 9 February 2023
0920-3796/© 2023 The Author(s). Published by Elsevier B.V. This is an open access article under the CC BY-NC-ND license (http://creativecommons.org/licenses/by-nc-nd/4.0/).

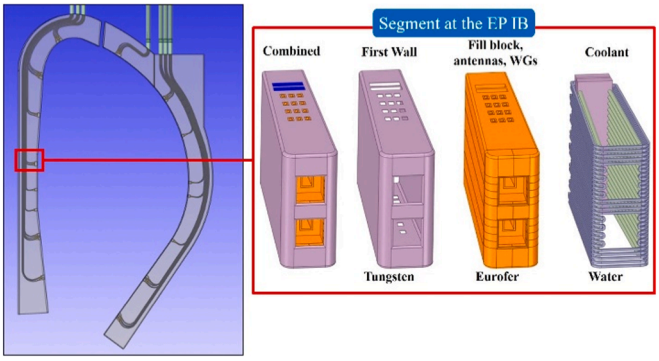

Fig. 1. Location of the DSC under investigation and its components.

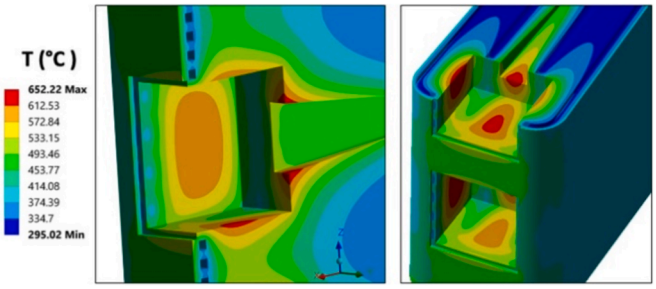

Fig. 2. Temperature distribution in EUROFER from previous work [8].

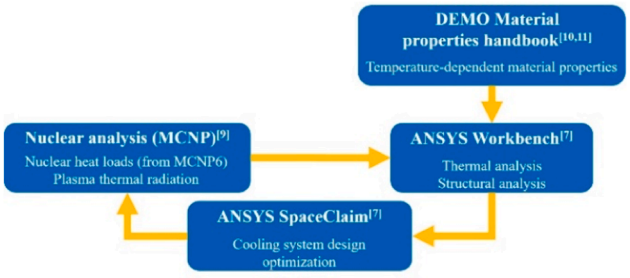

Fig. 3. Workflow and simulation tools.

imported as inputs for calculations presented in this paper.

In order to properly model the expected operation conditions, temperature-dependent material properties were imported from the DEMO material properties handbooks [11,12] (perfect contact was assumed between solid materials) into ANSYS Workbench, which was then used to perform coupled thermal and computational fluid dynamics (CFD) analyses (ANSYS Mechanical and ANSYS CFX). The temperature distribution results were then used as boundary conditions in a structural analysis using ANSYS Workbench.

3. Coupled thermal analysis

The coupled thermal-CFD analysis was done using ANSYS workbench utilizing the system coupling module to transfer information between fluid-solid interfaces, following the procedure presented in [8].

In order to improve the cooling system performance around the antenna cavities, several modifications were done, following a trial and error approach at each optimization step (only the final configuration is shown here): 1) re-routing two of the cooling channels such that they pass closely above and below the antennas; 2) fold the cooling channels on the side of the cavities to reach the hotspots in the middle of the cavity side surfaces; 3) re-route two of the cooling channels to reach the hotspots of the cavity's top and bottom surfaces. These modifications are depicted in Figs. 4 and 5. Besides these geometrical changes, the material of the antennas was changed from EUROFER to tungsten, whose recrystallization temperature is 1300 °C [13].

The operating pressure and static temperature of the water coolant were set to Pressurized Water Reactor (PWR) inlet conditions (15.5 MPa, 295 °C), while the temperature-dependent thermo-physical properties of water were taken from the WCLL blanket design [14].

Using the updated cooling system configuration, the DSC module segment located at the equatorial plane IB is expected to have a maximum operating temperature of 657 °C in the tungsten FW layer, as shown in the left picture of Fig. 6. Note that this value is obtained in the surface surrounding the antenna; everywhere else, the temperatures are below 550 °C. The antennas themselves reach 581 °C, as presented on the right side of Fig. 6.

As for the EUROFER components of the DSC, the maximum operating temperatures are 541.08 °C and comply with the temperature limit for EUROFER under neutron irradiation, as shown in Fig. 7.

The maximum temperature reached by the water coolant is 326.4 °C (see Fig. 8), which is a 2 °C deviation from the coolant outlet temperature foreseen for the WCLL blanket (328 °C) [14]. This means that with this design the coolant will be close to the ideal outlet temperature for which the energy conversion system is optimized [15].

With the updated configuration the hotspots were removed everywhere except in the antennas, where it was not possible to bring the temperatures below 550 °C. As with the remaining plasma-facing components, this shows that the antennas need to be made of tungsten instead of EUROFER. This is not only because tungsten has a higher temperature limit, but also because it acts as a thermal shield for the EUROFER components behind it, which would also reach temperatures above 550 °C if the antennas were not made of tungsten. Additionally, the electrical conductivity of tungsten at this temperature is ~6 times higher than that of EUROFER [11,12], which means that the ohmic losses in the antenna will be reduced (although with a small impact on the performance of the system, as the antennas are very small components compared to the whole transmission lines). In addition, the tungsten erosion rate is 10 times lower than that of iron (the main component of EUROFER) [16], which means that tungsten antennas will retain their surface roughness, which affects the antenna efficiency.

4. Structural analysis

In order to evaluate the thermo-mechanical behaviour of the DSC module, a simplified geometry was prepared by removing the tungsten layer, simplifying fillets and corners, using symmetry boundary conditions in several locations [17,18] and reducing the size of the geometry to only a quarter of the DSC module (see Fig. 9).

The boundary conditions applied to the geometry were 1) symmetry in the poloidal direction on the top and bottom surfaces, to model the

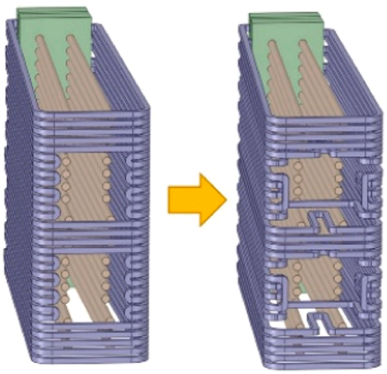

Fig. 4. DSC cooling system: previous design (left); updated design (right).

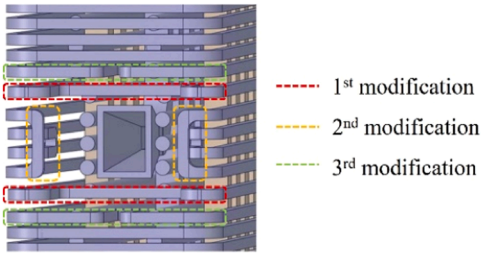

Fig. 5. Details of the modifications to the DSC cooling channels.

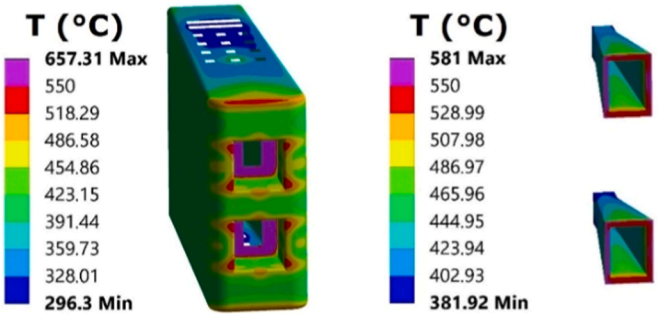

Fig. 6. Operating temperatures (°C) in tungsten. Left: in the sacrificial FW layer. Right: antennas.

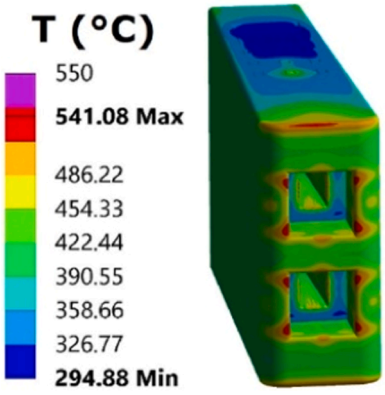

Fig. 7. Operating temperatures (°C) in EUROFER.

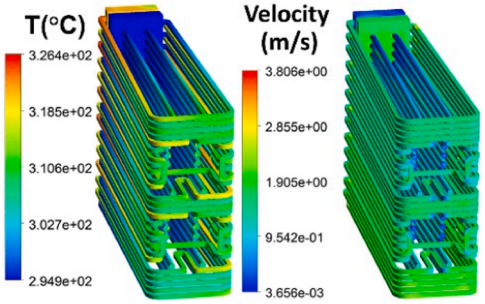

Fig. 8. Cooling system of the DSC. Left: Temperature distribution (°C). Right: Velocity distribution (m/s).

single module segment (SMS) structure of the DSC, and 2) symmetry in the toroidal direction, to model the other half of the DSC structure, as shown in Fig. 10 and following the boundary conditions applied in [17, 18]. A fixed support constraint was applied on the single middle edge located on the toroidal symmetry surfaces (see Fig. 11). This constraint

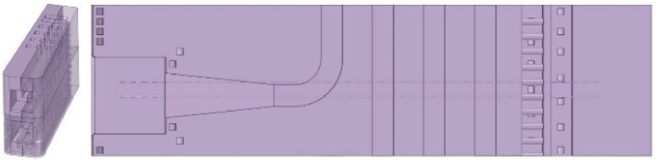

Fig. 9. The reduced geometry. Left: placed together with the original geometry (in transparency). Right: side view of the reduced geometry and its discontinuous region.

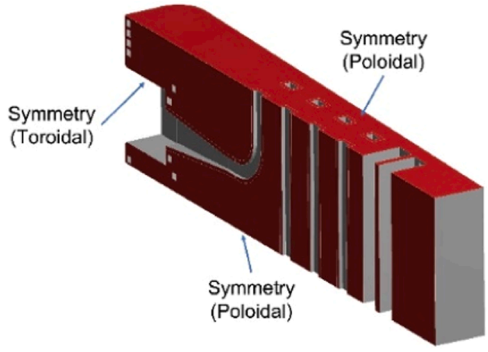

Fig. 10. Symmetry boundary conditions of the DSC module based on a sliced unit.

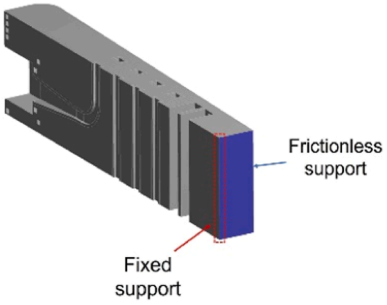

Fig. 11. Support boundary conditions of the DSC module based on a sliced unit.

models the unity of this geometry and its symmetry counterpart. Frictionless support was applied to the back surface of the geometry, to provide some degree of freedom on the poloidal direction, following [17] (see Fig. 11).

In order to calculate the primary stresses (P) and secondary stresses (Q) in the DSC, multiple loads were applied to the DSC following the elementary operation case of [19], which means that only thermo-mechanical loads, coolant pressure and gravity were considered. The gravity load was modelled by applying a standard earth gravity of 9.81 m/s^2. The coolant design pressure of 15.5 MPa was multiplied by a safety factor of 1.15, resulting in a total of 17.825 MPa applied to the

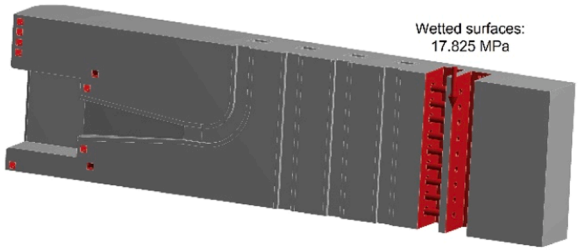

Fig. 12. Pressure load on the DSC module on a sliced unit.

wetted surfaces of the cooling channels inside the DSC module (see Fig. 12), following [20]. Finally, the temperature map from the thermal analysis (see Fig. 7) was imported as a thermal load.

The calculated equivalent Von Mises stress distribution of the $P + Q$ stresses is presented in Fig. 13. Direct observation reveals that the stress distribution is mostly concentrated in the antenna apertures, due to the temperature levels. The other factor affecting these results is the temperature gradients between surfaces, as steeper temperature gradients induced higher stresses. This is the reason why the locations of the maximum stresses are not exactly the same as the locations of the maximum temperatures.

We followed the procedure of [21] to assess the thermo-mechanical loads based on the Stress Linearization (SL) of the stress tensor on a path defined along the thickness of a region where the Von Mises stresses are higher. Therefore, the critical areas in the DSC module geometry were identified by looking closely to the Von Mises stress field presented in Fig. 13. As expected, the region close to the plasma-facing component has the highest stresses and becomes the critical area.

The paths for stress assessment on the simplified geometry of the DSC module are presented in Fig. 14. To calculate the stress on these paths, line integration and stress breakdown were done inside ANSYS. In order to prevent Immediate Plastic Collapse (IPC), Immediate Plastic Instability (IPI) and Immediate Plastic Localization Flow (IPFL), the criteria in Table 1 was used. The stress assessments with regard to the Règles de Conception et de Construction des Matériels Mécaniques des îlots nucléaires RNR (RCC-MR) level A criteria are presented in Fig. 15.

The results of the stress linearization for IPC and IPI are in line with the results of the cases presented in [23] for the WCLL BB on similar paths. This is expected, since the dimensions of the FW cooling channels were adopted from the WCLL design. Regarding the IPFL test, the results show that the current design is expected to withstand the primary and secondary loads without compromising the structural integrity of the DSC. Furthermore, since the results presented comply with the RCC-MR level A criteria, the safety of the components for the specified operation throughout the DSC lifetime is ensured.

5. Conclusions and future work

A thermo-mechanical study was performed for a section of the DSC located on the high-field side at the equatorial plane aiming to ensure operating temperatures below the material limits under irradiation. This design was then optimized using steady-state coupled thermal-CFD analyses, performed with ANSYS Workbench. Previous work had shown that though the cooling system design managed to keep most of the DSC temperature below 550 °C, there were hotspots around the antenna cavities with temperatures of 652 °C.

Further iterations on the cooling channel design of the DSC, which focused on the hotspots, showed that it is not possible to maintain the operating temperatures below 550 °C when the antennas of the DSC are made of EUROFER. Therefore, tungsten, which will also be used in the 2 mm plasma-facing layer of the DEMO BB, is proposed to replace EUROFER in the antennas. This is because tungsten has a higher temperature limit (1300 °C) than EUROFER and, besides, will act as a thermal shield for the EUROFER behind it.

According to the simulation results presented in this work, the updated design of the DSC cooling channels is able to keep the DSC maximum temperatures within the limits: 541 °C in the EURODER structure, 657 °C in the tungsten layer, and 581 °C in the antennas. These results clearly show the effectiveness of the new cooling channel design and the use of tungsten in the antennas. Additionally, the maximum velocity of the coolant is just half of the maximum allowable coolant velocity to avoid erosion and the outlet temperature of the water coolant is only 2 °C below the desirable outlet water temperature, which is important because the power conversion system of DEMO is optimized for PWR conditions.

Using the temperature maps obtained in the thermal analysis, a structural integrity assessment was performed using a quarter of the updated DSC module and symmetry boundary conditions, both under normal operation and after long irradiation periods. The thermo-

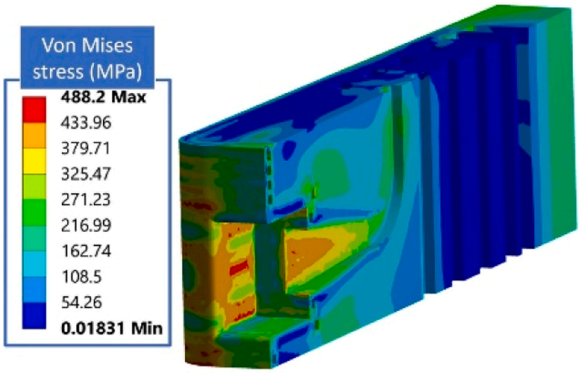

Fig. 13. Equivalent von Mises stress (MPa) of the sliced unit of the DSC module.

Fig. 14. Layout of the stress linearization path.

Table 1
P-type damage structural criteria summary [22].

Damage	Quantity	Limit criteria Level A	Level D
IPC	$\overline{P_m}$	S_m^A	S_m^D
IPI	$\overline{P_L + P_B}$	$1.5S_m^A$	$1.5S_m^D$
IPFL	$\overline{P_L + Q_L}$	$3S_m^A$	No limit

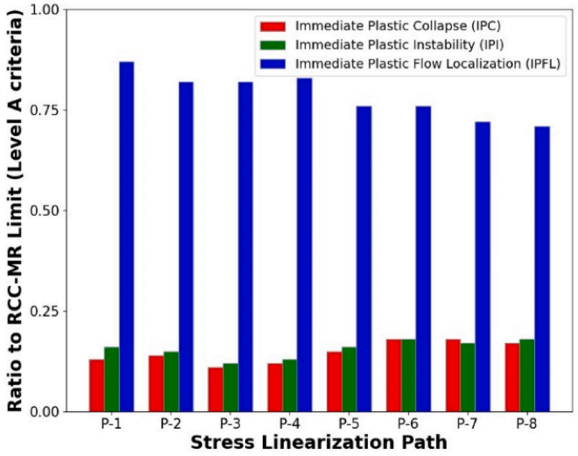

Fig. 15. Results of stress linearization of the critical region compared with RCC-MR level A criteria.

mechanical assessment under normal operation allowed to conclude that the current design already complies with the RCC-MR level.

With the current assumptions, the proposed cooling system is able to keep the DSC operating temperatures within the limits without compromising the mechanical integrity of the system. This work should be extended in the future to include material fatigue and cyclic (S-type) loads.

This work shows that the plasma-facing components of nuclear fusion reactor diagnostics should be carefully designed, with sufficient cooling and materials with high thermo-mechanical performance, in order to withstand the nuclear, thermal and mechanical loads in the harsh radiation environment inside the vessel.

Declaration of Competing Interest

The authors declare that they have no known competing financial interests or personal relationships that could have appeared to influence the work reported in this paper.

Data availability

No data was used for the research described in the article.

Acknowledgements

This work has been carried out within the framework of the EUROfusion Consortium, funded by the European Union via the Euratom Research and Training Programme (Grant Agreement No 101052200 — EUROfusion). Views and opinions expressed are however those of the author(s) only and do not necessarily reflect those of the European Union or the European Commission. Neither the European Union nor the European Commission can be held responsible for them. IST activities also received financial support from Fundação para a Ciência e Tecnologia (FCT) through the individual grant PD/BD/135230/2017 under the APPLAuSE Doctoral Program.

References

[1] W. Biel, et al., Diagnostics for plasma control – From ITER to DEMO, Fusion Eng. Des. 146 (2019) 465–472.
[2] W. Biel, et al., Development of a concept and basis for the DEMO diagnostic and control system, Fusion Eng. Des. 179 (2022), 113122.
[3] G. Federici, et al., An overview of the EU breeding blanket design strategy as an integral part of the DEMO design effort, Fusion Eng. Des. 141 (2019) 30–42.
[4] F. da Silva, et al., Benchmarking 2D against 3D FDTD codes for the assessment of the measurement performance of a low field side plasma position reflectometer applicable to IDTT, JINST 17 (2022) C01017.
[5] A. Malaquias, et al., Integration Concept of the Reflectometry Diagnostics for the Main Plasma in DEMO, IEEE Trans. Plasma Sci. 46-2 (2018) 451–457.
[6] R. Lässer, et al., Strucutral materials for DEMO: the EU development, strategy, testing and modelling, Fusion Eng. Des. 82 (2007) 511–520.
[7] ANSYS®, Academic Research Mechanical, Release 19.1, 2018. Canonsburg, PA, USA.
[8] Y. Nietiadi, et al., Nuclear and thermal analysis of a multi-reflectometer system for DEMO, Fusion Eng. Des. 167 (2021), 112349.
[9] R. Luís et al. Nuclear and Thermal Analysis of a Reflectometry Diagnostics Concept for DEMO, IEEE Trans. Plasma Sci. 46:5 (2018) 1247-1253.
[10] J.T. Goorley, et al., Initial MCNP6 Release Overview - MCNP6 Version 1.0, 2013.
[11] E. Gaganidze et al., *Material Properties Handbook – EUROFER97*, Eurofusion IDM reference: EFDA_D_2NZHBS, 2020.
[12] E. Gaganidze, et al., Material Properties Handbook - Tungsten, 2020. Eurofusion IDM reference: EFDA_D_2P3SPL.
[13] S. Nogami, et al., *Degradation of tungsten monoblock divertor under cyclic high heat flux loading*, Fusion Eng. Des. 120 (2017) 49–60.
[14] A. Del Nevo, et al., WCLL design report 2017, in: , 2017.
[15] F. Giannetti, et al., BB/DIV/VV PHTS and Power Conversion System (PCS) Preliminary Design (DDD), 2020. Eurofusion IDM reference: EFDA_D_2N9MAE.
[16] M.Z. T.okar, M. Beckers, W. Biel, Erosion of installations in ports of a fusion reactor by hot fuel atoms, Nucl. Mater. Energy 12 (2017) 1298–1302.
[17] A. Retheesh, F.A. H.ernández, G. Zhou, Application of Inelastic Method and Its Comparison with Elastic Method for the Assessment of In-Box LOCA Event on EU DEMO HCPB Breeding Blanket Cap Region, Appl. Sci. 11 (2021) 9104.
[18] R. Forte, et al., Preliminary design of the top cap od DEMO Water-cooled Lithium Lead breeding blanket segments, Fusion Eng. Des. 161 (2020), 111884.
[19] M. Utili, et al., Load Specification Document, 2020. Eurofusion IDM reference: EFDA_D_2P86SX.
[20] G.A. S.pagnuolo, et al., Development of load specifications for the design of the breeding blanket system, Fusion Eng. Des. 157 (2020), 111657.
[21] AFCEN, RCC-MRx: Design and construction rules for mechanical components of nuclear installation, Addenda Included (2013), 2013. Paris, France.
[22] G. Slagis, ASME Section III Design-by-Analysis Criteria Concepts and Stress Limits, ASME J. Pressure Vessel Technol. 128 (2006) 25–32.
[23] I. Catanzaro, et al., Parametric study of the influence of double-walled tubes layout on the DEMO WCLL breeding blanket thermal performances, Fusion Eng. Des. 161 (2020), 111893.